Turkish Journal of Electrical Engineering & Computer Sciences

http://journals.tubitak.gov.tr/elektrik/

Research Article

Turk J Elec Eng & Comp Sci
(2016) 24: 3949 – 3960

doi:10.3906/elk-1412-169

An HF/UHF dual mode RFID transponder antenna and HF range extension using UHF wireless power transmission

Mustafa Murat BİLGİÇ[1], **Korkut YEĞİN**[2,*]
[1]Unitest Inc., İstanbul, Turkey
[2]Department of Electrical and Electronics Engineering, Ege University, İzmir, Turkey

Received: 26.12.2014 • **Accepted/Published Online:** 25.06.2015 • **Final Version:** 20.06.2016

Abstract: An HF/UHF compatible RFID transponder antenna is designed, simulated, and measured for dual band operation and HF range extension. A dual mode compatible RFID transponder antenna has the benefits of each mode and eliminates the disadvantages of single mode operation. One of the major drawbacks of UHF antennas is their poor performance when the tag is placed on or near metallic objects. To overcome this shortcoming, two-layer substrate with degenerate grounded is used and a 4-turn spiral antenna is placed on the top and bottom parts of the substrate for HF operation. The co-existence of both antennas affects standalone performances but desired specifications can be achieved with the proposed design. A prototype is built and measured to verify the target design criteria. Measured inductance of the HF loop is 2.54 μH and the gain of the UHF antenna is 2.73 dBi when placed on a metallic can. The transponder antenna can be configured for HF mode, UHF mode, or HF with range extension through a wireless power transmission (WPT) using the UHF band. WPT at the UHF band provides additional DC voltage for HF tag operation. This relatively new idea of HF range extension is supported with simulations and basic measurements.

Key words: HF RFID, UHF RFID, dual mode tags, multiband RFID, wireless power transmission, range extension

1. Introduction

Radio-frequency identification (RFID) systems are important for many applications in consumer electronics, logistics, and manufacturing companies to provide information about the products, people, and animals. The energy and data-exchange are provided by using magnetic, electric, or electromagnetic fields. The data carrying device is usually termed the transponder or tag, and the reader sends power and clock signals to establish one-way or two-way communication. Compared to other autoidentification systems, RFID has a larger distance between the data carrier and the reader, very fast response time ($<$1 s), and exchange of high data quantities, which, in turn, also enables secure communication and precludes unauthorized copying of the data carrier [1].

One of the most commonly used RFID systems is HF RFID because it is cost effective, easy to realize, and durable against harsh environments such as on or near metallic and dielectric surfaces, because magnetic field lines do not undergo significant change over short distances. On the other hand, they have limited read/write range capability since magnetic field lines created between the interrogator antenna and the tag antenna decay rapidly ($\sim r^{-3}$).

The UHF band provides much larger bandwidth and higher data rates, which can be utilized for resolving security and authentication issues, and more read/write range compared to HF RFID. However, UHF tags can

*Correspondence: yegink@gmail.com

easily be affected by the application environment such as on/near metal and plastics. When tags are placed in such environments, tag impedance can change and detune easily, and also radiation characteristics may change considerably, which, in turn, makes the UHF tag less reliable. There has been considerable effort to improve the performance of UHF RFID tags on or near metallic surfaces [2–9]. Recently, near-field UHF RFID systems have also gained attraction, but read-range is limited to a few centimeters, which precludes their use for applications where the transponder tag is physically located at a much larger distance from the reader.

It is also possible to design a dual band, HF and UHF compatible RFID tag since they complement each other in many ways. The idea of dual band RFID has been first exploited in using a printed dipole and a multiturn loop [10]. The printed dipole was intended for UHF and the multiturn loop was dedicated for HF. However, the UHF design suffers degradation when the tag is placed on/near a metallic surface. Actually, dipole-like UHF structures are prone to such degradation. Maybe the most notable study for dual band operation was carried out by Mayer and Scholtz [11]. The designed tag antenna and chip was capable of operating at 13.56 MHz and at 868 MHz. The antenna was a single feed for dual operation; hence it was different than previous dual band designs. For the HF band, a spiral antenna was used as usual. The gain of the slot antenna at the UHF band was stated as –4.69 dBi. Another study on dual band tag design was reported by Iliev et al. [12]. The antenna was a dipole-like structure with a gain of –2.3 dBi in free space. Resonance for HF was achieved at 16.1 MHz with a quality factor of 10.1. Other dual band designs have also been reported [13–17], but all of them suffer performance degradation of UHF RFID near or on metallic objects due to the inevitable nature of the antenna structure being used.

The main bottleneck in RFID antenna design is the cost associated with the antenna part. Due to this constraint most designs are limited to planar antennas imprinted on low-cost substrate. However, it is an undisputable fact that these designs do not exhibit good, reliable performance at the UHF band when the transponder is placed on metal-like structures. At the expense of cost, there is a need for a dual band, HF and UHF compatible RFID tag that is not affected by its environment, especially by metallic objects, and yet still provides adequate gain for seamless operation. In addition, it is also possible to extend the range of the HF tag by sending wireless power through the UHF band. Additional power can be sent from the reader in the UHF band, and that power can be utilized by the HF tag. Although the maximum range for HF operation cannot be regarded as the true far-field for UHF operation, being outside the reactive zone of the UHF tag, it is possible to transmit power to the tag. Since the tag is dual band, the UHF portion of the tag rectifies the received RF power in the UHF band and supplies the HF IC for increased read range. Thus, the novelties of the proposed design are dual band HF/UHF tag antenna design, near-metallic operation of the UHF tag antenna, and UHF power transmission for the purpose of HF range extension. The reader antenna designs for HF and UHF bands are also performed and simple experiments have been carried out to prove this new concept.

2. Dual band transponder antenna design

A dual band RFID transponder antenna must fulfill the specifications for both HF and UHF applications. The target system performance is summarized in Table 1. Since both antennas share the same package, typical HF tag dimensions are selected as the package size. Required HF inductance for a typical 30–50 cm read range is taken as 2–3 μH [2,15–17]. For the UHF antenna, a Texas Instruments UHF STRAP 08 tag IC is chosen as reference and the antenna impedance is targeted to match that particular impedance, which is not 50 Ω. Similar to a dipole-like UHF tag antenna, minimum gain of 2 dBi is set as the target.

Table 1. Target specifications.

	HF	UHF
Frequency	13.56 MHz	865–868 MHz
Inductance	2–3 μH	-
Input impedance	-	35+j165 Ω
Gain	-	min 2 dBi
Size	$< 95 \times 95$ mm^2	
Standard	ISO 14443	ISO 18000-6

The antenna structure is composed of a 4-turn HF loop and a patch antenna with degenerate ground. One turn of the HF loop is on the upper substrate and the remaining three turns are located on the lower substrate. Degenerate ground helps to achieve the target input impedance and improves the gain of the antenna by modifying ground currents. A cross-shaped slot is used because it is easy to tune the slot arms to get the desired characteristics. The structure of the dual mode tag antenna is shown in Figure 1. The equivalent circuit model of the HF loop and the reader loop is illustrated in Figure 2.

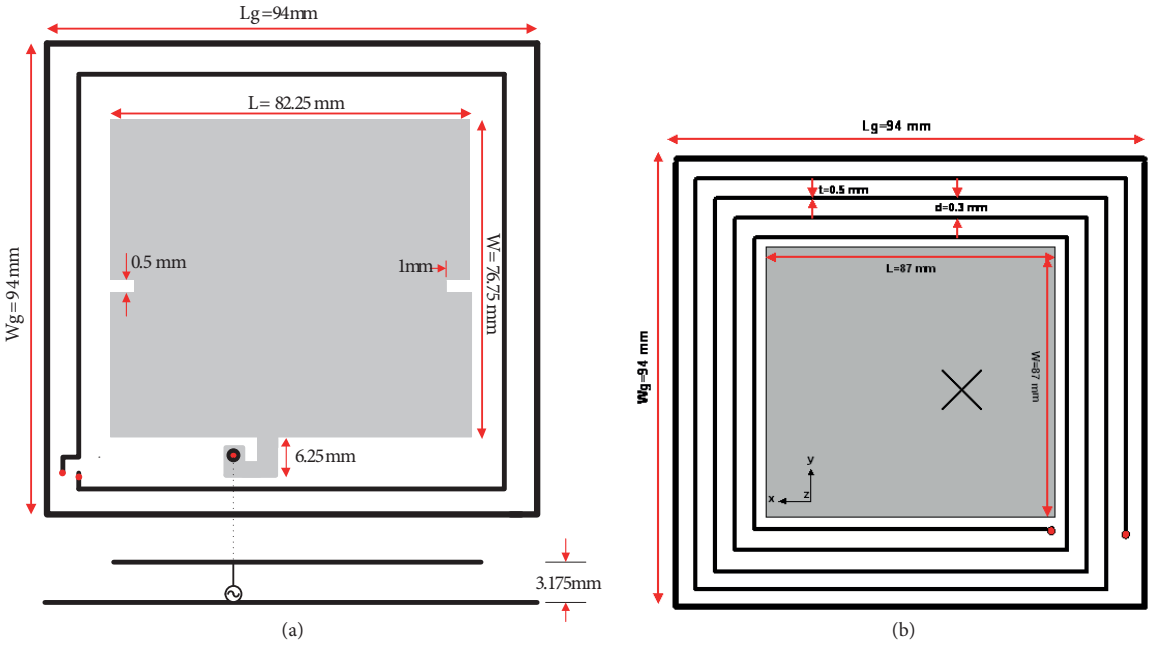

Figure 1. Proposed dual band transponder antenna (not to scale), a) top, b) bottom.

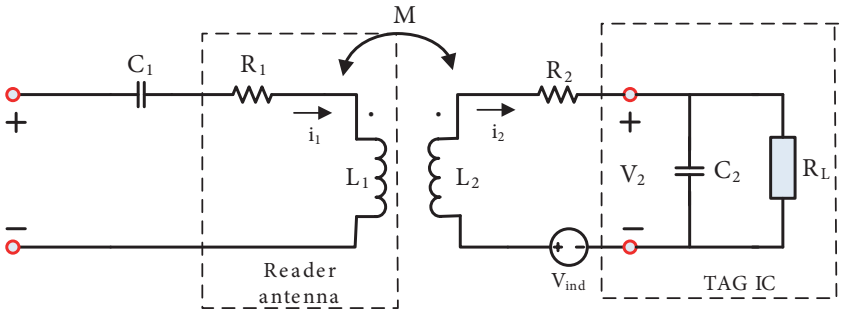

Figure 2. Equivalent circuit model for HF link.

It can be shown that the induced voltage on the HF part of the transponder tag is given as

$$V_2 = \omega \mu_0 \left| H_0 \right| S_2 N_2 Q, \tag{1}$$

where V_2 is the tag IC voltage, H_o is the required magnetic field intensity, N_2 is the numbers of turns needed on the tag, S_2 is the loop area of the tag, Q is the quality factor, ω represents the angular frequency, and μ_o is the permeability of free space. Q can be expressed as

$$Q = \frac{1}{R_2 \sqrt{\frac{C_2}{L_2} + \frac{1}{R_L}\sqrt{\frac{L_2}{C_2}}}} = \frac{1}{\frac{R_2}{\omega L_2} + \frac{\omega L_2}{R_L}}. \tag{2}$$

Once the minimum operating voltage for the tag IC is specified, the required magnetic field strength ($|H_o|$) from the reader coil can be found. That magnetic field should not exceed 132 dBμA/m (5 A/m) at the reader coil surface. ISO 15693 standard sets 42 dBμA/m at 10 m from the reader coil but this leads to much higher input ampere-turns and larger near field (28.2 A/m), which is not acceptable in many regulations set by the governing countries.

The microstrip patch antenna is fed from the edge. The substrate is Taconic RF 43 ($\varepsilon_r = 4.3$, $\tan\delta = 0.0033$). The parasitic effects of spiral turns on the UHF antenna are mainly on the radiation characteristics of the antenna. Both HF and UHF tag ICs can be placed on the top substrate and are located close to each other to facilitate RF to DC energy conversion. The prototype of the antenna is shown in Figure 3.

Figure 3. Prototype of the dual band transponder antenna.

3. HF transponder antenna simulations and measurements

3.1. Quasi-static inductance

The inductance of a rectangular spiral can be empirically calculated as [1]

$$L_{ind} = N^2 \frac{\mu}{\pi} \left[-2\left(W + L\right) + 2\sqrt{L^2 + W^2} - L \ln\left(\frac{L+\sqrt{L^2+W^2}}{W}\right) \right. \\ \left. -W \ln\left(\frac{W+\sqrt{L^2+W^2}}{L}\right) + L \ln\left(2L/a\right) + W \ln\left(2W/a\right) \right], \tag{3}$$

where N, W, L, a, and μ represent number of turns, width of the spiral, length of the spiral, wire radius, and magnetic permeability of the medium, respectively. The magnetic field of the axis of the rectangular loop can be expressed as

$$B_z = \frac{\mu I W L}{4\pi\sqrt{\left(\frac{W}{2}\right)^2 + \left(\frac{L}{2}\right)^2 + R^2}} \left[\frac{1}{\left(\frac{W}{2}\right)^2 + R^2} + \frac{1}{\left(\frac{L}{2}\right)^2 + R^2}\right], \tag{4}$$

where I and R represent the input current to the loop and the distance from the center of the loop, respectively. These approximate formulas have been derived from quasi-static relations and do not include the mutual coupling between the turns or interwinding capacitances. Using (3), the inductance of the HF loop in air is calculated as 7.76 μH.

3.2. Simulations and measurements of HF coil

When the dual band tag is simulated with FEKO (3D electromagnetics field solver), the inductance is found as 3.37 μH due to the presence of top and bottom metallization and substrate. Then the loop is measured with a network analyzer (Rohde & Schwarz ZVB-20) and the measured inductance at 13.56 MHz was 2.54 μH. The discrepancy was mainly attributed to inadequacies in low-frequency solution of the problem as the structure appears to be electrically too small at the HF band. Measured, simulated, and analytical HF loop inductances are displayed in Figure 4.

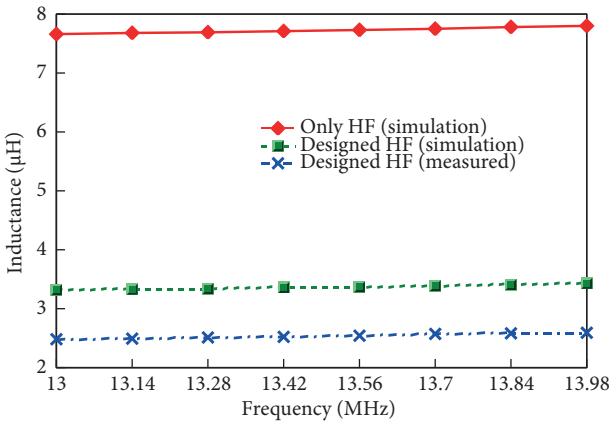

Figure 4. HF antenna inductance (simulated in free space, simulated dual band, measured dual band).

3.3. HF range extension

A representative reader coil is also designed using a three-turn spiral with 35 × 25 cm ($L \times W$) dimensions and 0.5-mm diameter wire to get 12.1 μH inductance using (3). The reader coil is built and measured with a network analyzer. The measured inductance was 12.3gμH. Then this reader is co-axially placed on the transponder antenna starting from 25 cm to 110 cm in simulations. Input ampere-turns to the reader coil are taken as 1.596 to get 5 A/m maximum near-field and 0.639 to get 2 A/m, which is a more typical value in current readers. Induced voltage on the transponder HF coil is calculated using (1) and (4). The loaded Q of the transponder tag is taken as 30 and voltage conversion efficiency of 80% is assumed on the rms value of the induced voltage to get the rectified DC voltage. Magnetic field intensities and expected DC voltages are shown in Table 2. If the minimum operating voltage for the tag IC is assumed to be 2.5 V, then the analysis indicates

50 cm and 75 cm range for 0.639 and 1.596 ampere-turns reader coil, respectively. Thus, any power transfer using the UHF link must compensate for the voltage difference to operate the HF tag. For example, the normal HF range of 50 cm for 0.639 ampere-turns can be extended to 80 cm if 1.63 VDC is obtained from the UHF link through RF-DC conversion.

Table 2. HF tag rectified voltage.

	0.639 Amp-turns		1.596 Amp-turns	
R (cm)	H (mA/m)	V_{DC} (V)	H (mA/m)	V_{DC} (V)
0	2000	-	5000	-
25	317.7	17.062	793.6	42.616
30	214.2	11.500	534.9	28.723
35	149.2	8.013	372.7	20.014
40	107.2	5.758	267.8	14.382
45	79.2	4.253	197.8	10.623
50	59.9	**3.218**	149.7	8.039
55	46.3	2.487	115.7	6.213
60	36.5	1.959	91.1	4.892
65	29.2	1.567	72.9	3.915
70	23.7	1.273	59.2	3.179
75	19.5	1.047	48.7	**2.614**
80	16.2	0.870	40.5	2.174
85	13.6	0.731	34.0	1.827
90	11.5	0.620	28.8	1.549
95	9.9	0.530	24.7	1.325
100	8.5	0.457	21.2	1.141
105	7.4	0.396	18.4	0.990
110	6.4	0.346	16.1	0.864

4. UHF transponder antenna simulations and measurements

The UHF antenna must not only comply with the specifications stated in Table 1, but also be operable when placed on or nearby metallic objects and liquids. Most UHF RFID transponder antennas utilize dipole-like structures with capacitive feed or T-feed to get the desired input impedance [18]. One of these designs, the Texas Instruments TI RI UHF STRAP 08 antenna, is taken as reference for our simulations. The reference antenna is modeled in FEKO and shown in Figure 5. Free-space simulations of the designed tag antenna and reference antenna in terms of directivity and input impedance are summarized in Table 3. Since the input impedance of tag IC is not at 50 Ω, the input impedance of the patch antenna is optimized to match this tag impedance for maximum power transfer. The radiation pattern of the designed antenna is shown in Figure 6. When this reference antenna is used on nonmetallic structures, its performance is robust. Other dipole-like UHF RFID antennas exhibit similar performance as well.

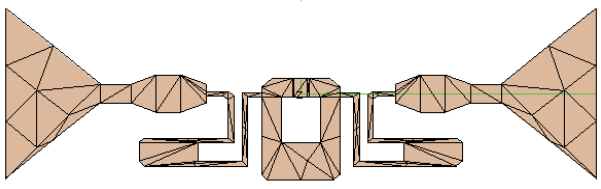

Figure 5. TI RI UHF STRAP 08 antenna model.

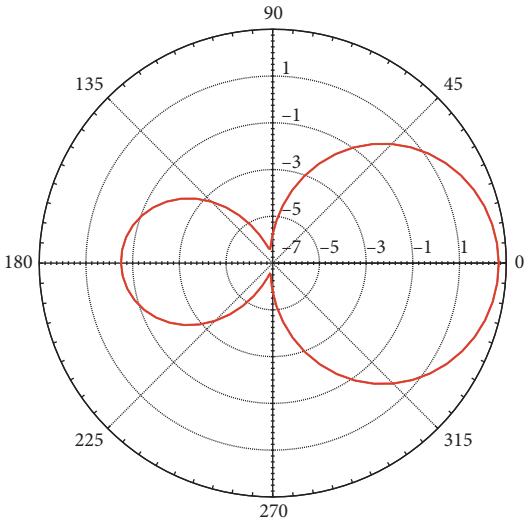

Figure 6. UHF tag antenna co-pol radiation pattern at 868 MHz.

Table 3. Simulation comparison of reference antenna and designed antenna.

Freq. (MHz)	D_{patch} (dBi)	D_{Ref} (dBi)	Z_{patch} (Ω)	Z_{Ref} (Ω)
861	2.46	1.89	17.1+j124.7	35.8+j44.3
862	2.50	1.89	18.7+j128.9	34.7+j44.5
863	2.54	1.89	20.5+j133.3	33.6+j44.8
864	2.56	1.89	22.5+j138.1	32.6+j45.1
865	2.61	1.89	25.0+j143.3	31.6+j45.4
866	2.63	1.89	27.8+j149.0	30.6+j45.3
867	2.66	1.89	31.2+j155.1	29.7+j46.1
868	2.68	1.89	35.1+j161.9	28.8+j46.4
869	2.70	1.89	39.9+j169.3	28.0+j46.8
870	2.72	1.90	45.6+j177.5	27.2+j47.2
871	2.74	1.90	52.7+j186.5	26.4+j47.6

A dual band RFID transponder antenna was placed on a cylindrical metallic can with 80 mm diameter and 120 mm height as shown in Figure 7. Simulated and measured results of input impedance (resistance and reactance) are shown in Figure 8. In the simulation model, the antenna was placed at the center on top of the can and was displaced about 0.125 mm above the metallic surface to simulate the presence of a dielectric cover. Although there is some discrepancy between the measured and simulated results, the worst relative error within the target bandwidth is less than 13.2% and the measured results displayed less variation than simulated ones.

We also performed simulations with the reference antenna on the same structure; again the reference antenna was elevated 0.125 mm above the top surface. Comparison of simulated results between the proposed structure and reference antenna is displayed in Table 4. As expected, the input impedance of the reference antenna changed drastically to lower values, while its directivity increased as radiated energy was directed to the broadside. On the other hand, the proposed antenna has considerably less degradation when placed on a metallic can.

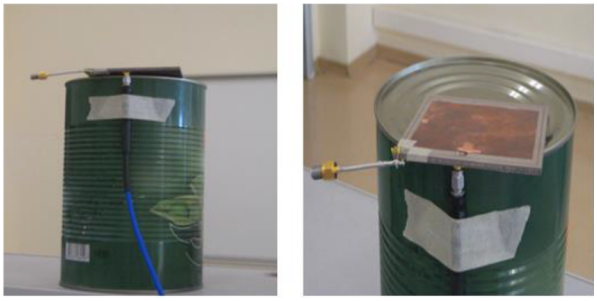

Figure 7. Measurement setup for antenna on metallic can.

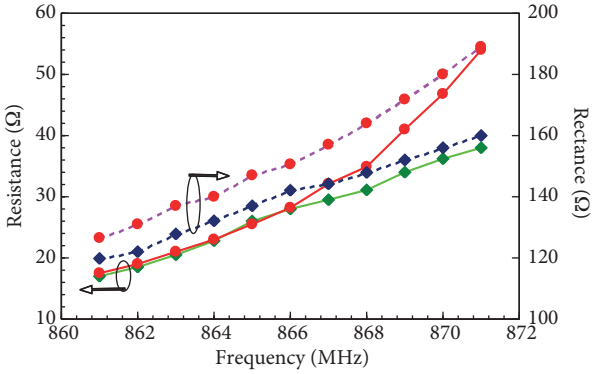

Figure 8. Resistance and reactance of input impedance (measured and simulated).

Table 4. Simulation comparison of reference antenna and designed antenna on a metallic can.

Freq. (MHz)	D_{patch} (dBi)	D_{Ref} (dBi)	Z_{patch} (Ω)	Z_{Ref} (Ω)
861	2.50	2.48	17.5+j126.3	0.01+j67.4
862	2.56	2.48	19.0+j130.4	0.01+j67.5
863	2.59	2.49	20.8+j134.9	0.01+j67.6
864	2.63	2.51	22.9+j139.7	0.01+j67.7
865	2.67	2.53	25.4+j145	0.01+j67.8
866	2.70	2.55	28.2+150.6	0.01+j67.9
867	2.72	2.58	31.7+157	0.01+j68
868	2.75	2.59	35.7+163.8	0.01+j68.1
869	2.77	2.66	40.6+171.4	0.01+j68.2
870	2.79	2.69	46.6+179.7	0.01+j68.3
871	2.80	2.72	54+j189	0.01+j68.4

5. Wireless power transmission through UHF

Simulated results for the longest range of HF tag operation were 50 cm and 75 cm for 0.639 ampere-turns and 1.569 ampere-turns, respectively (Table 2). Then required voltages (ΔV) that should be obtained through UHF RF-to-DC conversion are presented in Table 5 for minimum 2.5 VDC operation voltage.

If G_t represents the UHF reader antenna transmit gain and G_r the UHF tag antenna receive gain, then the received power (P_r) at the far field can be estimated using Frii's formula under matched load condition. Thévenin open circuit voltage under matched load condition can be calculated as

$$V_{oc} = \sqrt{8P_r\, R_{ant}}, \tag{5}$$

where R_{ant} represents the resistance of the receive antenna input impedance.

To simulate and measure WPT, we designed a 3-element Yagi-Uda antenna as the UHF reader antenna with 7.8 dBi simulated gain. The antenna is realized and shown in Figure 9, where the feed element has $\lambda/4$ balun. Measured antenna gain was 7.2 dBi.

If the designed tag antenna (G_r = 2.68 dBi) is used with this UHF reader antenna (G_t = 7.8 dBi), open-circuit voltages under matched load condition at the tag antenna can be calculated for 0.5 W and 2 W transmit powers using (4). Induced voltages at the tag can also be numerically found using 3D simulation tool FEKO. Both results as tag-reader distance varied are shown in Table 6.

Table 5. Required additional voltages for HF tag operation.

	0.639 Amp-turns	1.596 Amp-turns
Distance (cm)	ΔV required (V)	ΔV required (V)
55	0.013	-
60	0.541	-
65	0.933	-
70	1.227	-
75	1.453	-
80	1.630	0.326
85	1.769	0.673
90	1.880	0.951
95	1.970	1.175
100	2.043	1.359
105	2.104	1.510
110	2.154	1.636

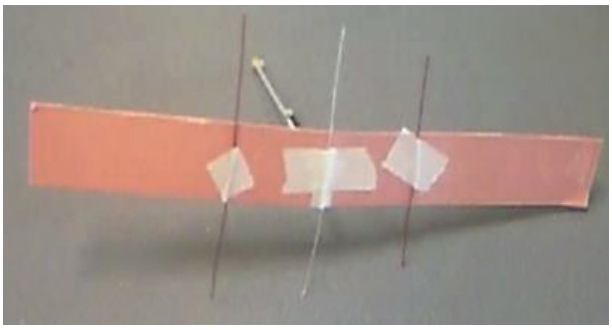

Figure 9. Three-element Yagi-Uda antenna for UHF reader antenna.

Table 6. Simulated open-circuit voltages induced through UHF.

	0.5 W		2 W	
Distance (cm)	$V_{OC,Friis}$ (mV)	V_{sim} (mV)	$V_{OC,Friis}$ (mV)	V_{sim} (mV)
50	2176.24	2346.18	4352.47	4682.46
55	1978.40	2157.38	3956.79	4304.87
60	1813.53	2006.06	3627.06	4002.22
65	1674.03	1868.18	3348.05	3727.87
70	1554.45	1737.36	3108.91	3466.24
75	1450.82	1626.35	2901.65	3244.21
80	1360.15	1515.33	2720.29	3022.88
85	1280.14	1410.68	2560.28	2814.99
90	1209.02	1318.75	2418.04	2630.44
95	1145.39	1227.54	2290.77	2448.71
100	1088.12	1138.44	2176.24	2271.23
105	1036.30	1057.83	2072.61	2111.42
110	989.20	982.17	1978.40	1960.10

Next we created a rectifier model using a single Schottky diode (HSMS 2822) with the model parameters shown in Table 7. The rectifier model is illustrated in Figure 10. The subcircuit in the model represented S-parameters of the reader (transmit) antenna and the transponder (receive) tag antenna, which was derived

from 3D electromagnetic simulations for each tag to reader separation. Shunt capacitance C_1 is only used for 2 W transmitted power.

Table 7. Diode model parameters.

Parameter	Value
Reverse saturation current (mA)	3.0×10^{-8}
Series resistance (Ω)	35
Reverse voltage capacitance (pF)	1.2
Breakdown voltage (V)	75
Temperature (°C)	26.85
Ideality factor	1

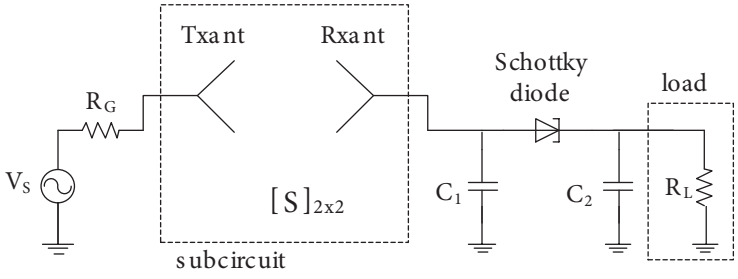

Figure 10. Single stage rectifier circuit ($C_1 = 0.5$ pF, $C_2 = 100$ pF, $R_L = 1.5$ kΩp.

The nonlinear characteristics of the diode give rise to different matching capacitance and load resistor values. The circuit is by no means the optimal circuit for voltage conversion efficiency, but it clearly shows that the desired DC voltages can be achieved with this single stage configuration. The output DC voltages of the rectifier for two different transmit powers are shown in Table 8.

Table 8. Simulated rectified DC voltages.

	2 W Transmit	4 W Transmit
Distance (cm)	VDC	VDC
55	1.299	4.217
60	1.486	4.117
65	1.138	3.730
70	1.699	3.299
75	1.302	3.140
80	1.380	2.870
85	1.056	2.660
90	0.828	2.830
95	0.663	2.300
100	0.857	2.061
105	0.534	1.990
110	0.428	1.870

6. Conclusions

An HF and UHF compatible dual band RFID transponder antenna is proposed and realized. Most UHF band RFID antennas utilize dipole-like structures and these antennas are known to exhibit poor characteristics

when placed on metallic or metal-like structures. To alleviate such environmental effects, a patch antenna with degenerate ground was proposed. Degenerate ground helped to tune the antenna to the desired input impedance of the tag IC. An HF loop antenna was placed on the top and bottom sides of the substrate. The UHF antenna was measured in free space and on a metallic can to show that its performance was considerably better than its dipole-like counterparts at the expense of two-metallic layer substrate. The inductance of the HF loop antenna was measured and it satisfied the target inductance criterion.

We also proposed wireless power transfer (WPT) through the UHF band to provide additional energy for the HF tag. With WPT, the working distance of the HF tag antenna for 0.639 ampere-turns can be increased from 50 cm to 70 cm and to 110 cm with 2 W and 4 W UHF transmit power, respectively. This alternative way of increasing HF read operation distance is quite new and can be useful in HF RFID applications.

References

[1] Finkenzeller, K. RFID Handbook: Fundamentals and Applications in Contactless Smart Cards and Identification. 1st ed. New York, NY, USA: John Wiley and Sons Ltd., 2003.

[2] Klapf Ch, Missoni A, Pribyl W, Holfer G, Holweg, G, Kargl W. Improvements in operational distance in passive HF RFID transponder systems. In: IEEE 2005 International Conference on RFID; 15–17 April 2005; San Diego, CA, USA. New York, NY, USA: IEEE. pp. 250-257.

[3] Nikitin PV, Rao KVS. An overview of near field UHF RFID. In: IEEE 2008 International Conference on RFID; 16–17 April 2008; Las Vegas, NV, USA. New York, NY, USA: IEEE. pp. 167-174.

[4] Rao KVS, Nikitin PV, Lam SF. Antenna design for UHF RFID tags: a review and a practical application. IEEE T Antenn Propag 2005; 53: 3870-3876.

[5] Cho C, Choo H, Park I. Design of planar RFID tag for metallic objects. Electron Lett 2008; 44: 175-177.

[6] Mo L, Zhang H, Zhou H. Broadband UHF RFID tag antenna with a pair of U slots mountable on metallic objects. Electron Lett 2008: 44: 1173-1174.

[7] Wonky C, Seong KJ, Hoon BJ. RFID tag antenna coupled by shorted microstrip line for metallic objects. Etri J 2008; 30: 597-599.

[8] Dobkin DM, Weigand SM. Environmental effects on RFID tag antennas. In: IEEE 2005 International Microwave Symposium; 12–17 June 2005; Long Beach, CA, USA; New York, NY, USA: IEEE. pp. 135-138.

[9] Arumugam D, Daniels WE. Characteristics of passive UHF RFID tags on metal slabs. In: IEEE 2009 APS-URSI International Symposium; 1–5 June 2009; Charleston, SC, USA; New York, NY, USA: IEEE. pp. 1-4.

[10] Park YK, Lee GS, Kang J, Chung YC. Various UHF RFID tags for metallic object. In: IEEE 2007 APS-URSI International Symposium; 10–15 June 2007; Honolulu, HI, USA; New York, NY, USA: IEEE. pp. 2285-2288.

[11] Mayer LW, Scholtz AL. A dual-band HF/UHF antenna for RFID tags. In: 2008 IEEE Vehicular Technology Conference; 21–24 September 2008; Calgary, BC, Canada; New York, NY, USA: IEEE. pp. 1-5.

[12] Iliev P, Thuck PL, Luxey C, Staraj R. Dual-band HF-UHF RFID tag antenna. Electron Lett 2009; 45: 439-441.

[13] Ma ZL, Jiang LJ, Xi J, Ye, TT. A single-layer compact HF-UHF dual-band RFID tag antenna. IEEE Antenn Wirel Pr 2012; 11: 1257-1260.

[14] Deleruyelle T, Pannier P, Egels M, Bergeret E. Dual band mono-chip HF-UHF tag antenna. In: IEEE 2010 APS-URSI International Symposium; 11–17 July 2010; Toronto, ON, Canada; New York, NY, USA: IEEE. pp. 1-4.

[15] Toccafondi A, Giovampaola CD, Mariottini F, Cucini A. UHF-HF RFID integrated tag for moving vehicle identification. In: IEEE 2009 APS-URSI International Symposium; 1–5 June 2009; Charleston, SC, USA; New York, NY, USA: IEEE. pp. 1-4.

[16] Toccafondil A, Braconi P. Compact meander line antenna for HF-UHF tag integration. In: IEEE 2007 APS-URSI International Symposium; 10–15 June 2007; Honolulu, HI, USA; New York, NY, USA: IEEE. pp. 5483-5486.

[17] Nishioka Y, Hitomi K, Okegawa H, Mizuno T, Fukasawa T, Miyashita H, Konishi Y. Novel antenna configuration for HF- and UHF-band hybrid card-type RFID tags. In: IEEE 2010 Antennas and Propagation (EuCAP); 12–16 April 2010; Barcelona, Spain; New York, NY, USA: IEEE. pp. 1-5.

[18] Dehollain C, Declercq M, Joehl N, Curty JP. Design and Optimization of Passive UHF RFID Systems. 1st ed. New York, NY USA: Springer, 2007.